International Journal of Innovative Scientific Research
2026, Vol. 4, Issue 4, pp. 6-20

International Journal of
Innovative Scientific Research

Journal homepage: https://ijisr.net

Research paper

Microclimate Dynamics Induced by Aircraft Landing and Takeoff Operations at Lubumbashi Luano International Airport (FZQA), Central Africa

Billy DIABASENGA KUSUAMINA [1] *, Albert KABASELE YENGA YENGA [1], Jean-Pierre FWAMBA MULUMBA [1], Stéphane MINGA MILOLO [1], André NZUZI NZUZI [2], Sion DIABASENGA LUYINDULA [3]

[1] *ETS, Ecole de Télédetection Spaciale, Doctoral School of Telecommunications and Space Remote Sensing, Department of Geomatics and Geodesy, Université Pédagogique Nationale, Kinshasa, Democratic Republic of the Congo*

[2] *Department of Physics and Applied Sciences, Faculty of Science, Université Pédagogique Nationale, Kinshasa, Democratic Republic of the Congo*

[3] *Civil Aviation Section, Institut Supérieur de Techniques Appliquées, Kinshasa, Democratic Republic of the Congo*

KEYWORDS

airport microclimate

landing and takeoff cycle

NDVI

surface artificialization

aviation safety

Lubumbashi

ABSTRACT

Background: Airports are coupled land–atmosphere–operations systems in which impervious surfaces, residual vegetation, boundary-layer variability, and concentrated aircraft activity interact across spatial and temporal scales. *Objective*: This expanded English-language secondary publication examines the microclimate of Lubumbashi/Luano International Airport (FZQA), a tropical high-elevation airport in the Democratic Republic of the Congo, and distinguishes structural surface warming from short-lived operational amplification. *Methods*: Hourly meteorological observations, Landsat and MODIS products, ERA5 reanalysis, CHIRPS precipitation, NASA POWER variables, terrain information, and air-traffic records are integrated through a surface-energy framework, an airport–reference land-surface-temperature contrast, a phase-weighted landing-and-takeoff exposure index, climatic stratification, difference-in-differences, and a confirmatory spatiotemporal model. *Results*: Available products indicate a persistent airport-related thermal core, an approximately 2.8 °C diachronic increase in surface temperature reported in the primary study, low vegetation abundance over artificialized surfaces, and greater detectability of operational thermal increments during the dry season and under weak-to-moderate winds. Aircraft operations are therefore interpreted as localized and transient amplifiers of a structurally warm surface rather than as the sole cause of warming. *Conclusion*: The framework supports airport environmental monitoring, density-altitude assessment, takeoff-performance analysis, low-level turbulence studies, and safety management, while defining the field measurements and uncertainty analysis required for doctoral-level causal validation.

1. Introduction

Airports are among the most intensively engineered land surfaces within modern transport systems. Runways, taxiways, aprons, terminal buildings, access roads, fuel facilities, and technical installations concentrate

***Corresponding author**: Billy DIABASENGA KUSUAMINA

DOI 105281/ijisr-2690826

CC BY SA

large areas of impervious materials within a relatively compact footprint. These surfaces alter radiative absorption, heat storage, roughness, runoff, and evapotranspiration, while aircraft engines, auxiliary power units, service vehicles, and recurrent landing-and-takeoff (LTO) cycles introduce additional mechanical and thermal forcing. The airport platform should therefore be treated as a coupled local-climate system rather than as a passive background surface.

Most aviation-climate research has addressed global radiative forcing, carbon dioxide emissions, and non-CO2 effects. Those global perspectives are essential, but they do not resolve the microscale and local-scale processes that develop within and immediately around an airport. Urban-climate research has shown that impervious materials, reduced vegetation, surface moisture deficits, and anthropogenic heat generate strong spatial heterogeneity in surface and near-surface temperature [16], [1], [17]. Thermal remote sensing has further demonstrated the usefulness of land surface temperature (LST) and vegetation metrics for identifying surface urban heat islands, while also warning that LST is not equivalent to canopy-layer air temperature [21], [15], [12].

Airport-specific evidence remains limited, particularly in tropical Africa. Gough and Leung [8] showed that many airport climate records exhibit peri-urban characteristics, supporting the idea that airports can create or reinforce a distinct local climate. Remote-sensing studies of Beijing Daxing International Airport found that large-scale construction and subsequent operations intensified the surface urban heat-island ratio within the surrounding landscape [23]. A recent assessment of Istanbul Airport likewise demonstrated that airport development can reorganize seasonal land-surface-temperature contrasts and the spatial distribution of heat-island intensity [25]. These studies establish the relevance of airport thermal environments but generally do not isolate short-duration operational forcing from the slower transformation of land cover. The Luano case addresses that gap by explicitly coupling surface structure, atmospheric modulation, and LTO timing.

The French-language primary publication [2] reported a persistent airport thermal signature, an approximately 2.8°C long-term increase in LST, a negative relation between vegetation abundance and temperature, stronger thermal contrasts during the dry season, and spatial coincidence between flight corridors and thermal hotspots. The purpose of the present English-language secondary publication is not to create new empirical observations. Instead, it (i) formalizes the coupled physical framework, (ii) presents a more explicit causal-identification strategy, (iii) introduces uncertainty and validation requirements, and (iv) expands the operational interpretation relevant to airport safety and planning.

The central hypothesis is that background warming at Luano is primarily controlled by surface artificialization and reduced vegetative cooling, whereas LTO activity produces spatially localized and temporally transient amplification. A scientifically defensible test of this hypothesis requires simultaneous control for radiation, rainfall, wind, season, time of day, surface type, and background urban conditions.

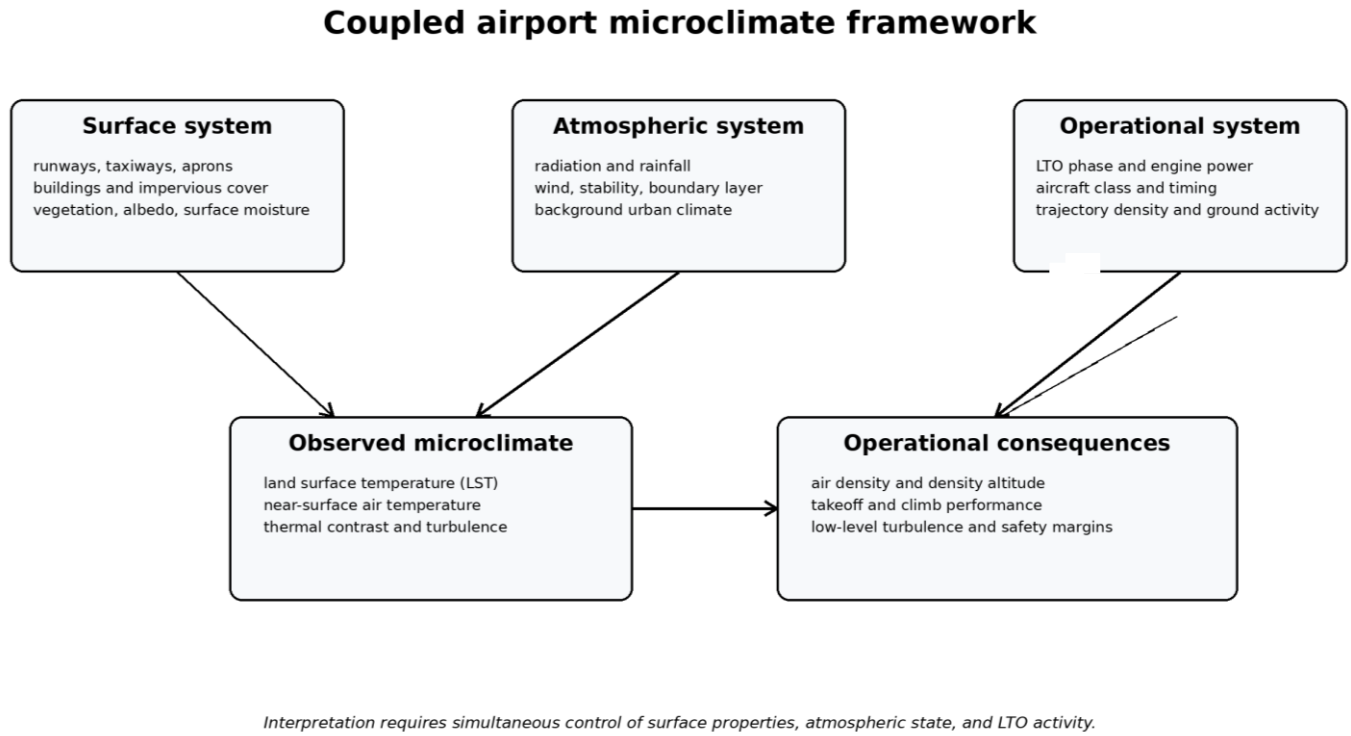

Fig. 1 Coupled surface-atmosphere-operations framework used to interpret the Luano airport microclimate. Surface characteristics generate the structural thermal background, atmospheric conditions regulate storage and dispersion, and LTO activity introduces localized thermal and mechanical pulses

The expanded contribution is fourfold. First, it distinguishes the structural airport heat-island component from the incremental operational component. Second, it formalizes a spatially explicit LTO exposure field rather than treating traffic as a single airport-wide count. Third, it embeds causal comparison within meteorological and biophysical controls. Fourth, it translates the conceptual findings into a confirmatory measurement and safety-relevant validation program suitable for tropical African airports.

2. Physical and Analytical Framework

2.1 Surface Energy Balance

Using a conventional positive-source sign convention, the airport surface energy balance may be represented as;

$$R_n + Q_f = H + LE + G + \Delta S \quad (1)$$

where R_n is net radiation, Q_f is anthropogenic heat release, H is sensible heat flux, LE is latent heat flux, G is conductive heat flux into the substrate, and ΔS is net heat storage. At an airport, Q_f includes building energy use, auxiliary power units, ground vehicles, engine exhaust, and high-power aircraft phases near the surface. Surface artificialization reduces evapotranspiration and therefore LE, while asphalt, concrete, and roofing materials can increase G and ΔS. The same net radiation can consequently produce a larger sensible-heat response than over vegetated reference surfaces.

2.2 Vegetation and Surface Thermal State

Vegetation abundance is represented by the normalized difference vegetation index (NDVI):

$$NDVI = (\rho_{NIR} - \rho_R)/(\rho_{NIR} + \rho_R) \quad (2)$$

where ρ_NIR and ρ_R are near-infrared and red reflectances. NDVI does not directly measure evapotranspiration or canopy temperature, but it provides a robust spatial indicator of vegetation abundance and photosynthetic activity. The inverse LST-NDVI relationship is well established in urban environments [22]. Surface albedo, moisture, emissivity, and material heat capacity must nevertheless be considered because identical NDVI values can coexist with different thermal responses.

2.3 Airport–Reference Thermal Contrast

The structural surface signal is summarized by an airport-reference contrast:

$$\Delta LST_t = mean(LST_A,t) - mean(LST_R,t) \quad (3)$$

where A denotes the airport footprint or an airport functional subzone and R denotes a physically comparable reference area. A positive and temporally persistent ΔLST indicates a structural surface anomaly. Because the result is sensitive to reference-zone definition, reference areas should be matched as closely as possible for elevation, regional climate, soil background, and distance from the urban core. The approach is analogous to satellite-based surface urban heat-island metrics [12], but the airport is treated as a distinct functional land system.

2.4 Spatial LTO Exposure

The original study introduced an LTO exposure index. A more explicit kernel representation is;

$$I_{LTO}(x,y,t) = \Sigma_i w_{p,i} w_{a,i} K[d_i(x,y); h] \quad (4)$$

where w_p,i is a phase weight for taxi, takeoff roll, initial climb, approach, landing, or deceleration; w_a,i is an aircraft or engine-class weight; K is a distance-decay kernel with bandwidth h; and d_i(x,y) is the distance between grid cell (x,y) and movement i. This index ranks potential operational exposure; it is not itself a temperature estimate. It provides a spatial prior for testing whether thermal anomalies align with repeatedly used operational corridors.

2.5 Difference-in-Differences and Covariate Control

A traffic-related increment cannot be inferred from a simple active-versus-idle comparison because active periods may also be warmer, drier, sunnier, or less windy. A difference-in-differences estimator is therefore appropriate:

$$\tau_DID = (Y_A,active - Y_A,idle) - (Y_R,active - Y_R,idle) \quad (5)$$

A regression implementation can be written as;

$$Y_z,t = \alpha + \beta_1\ Airport_z + \beta_2\ Active_t + \tau(Airport_z \times Active_t) + \gamma\text{^}T\ X_z,t + \mu_z + \lambda_t + \varepsilon_z,t \quad (6)$$

where Y may be LST or near-surface air temperature, X includes wind speed and direction, rainfall, net or shortwave radiation, humidity, NDVI, albedo, and surface moisture proxies, μ_z represents zone effects, and λ_t represents temporal controls. The coefficient τ is the conditional LTO-associated increment under the assumptions of the model. The source publication did not report a fitted value of τ; Eq. (6) is therefore presented as the formal estimation framework required for a future causal analysis, not as a retrospectively estimated result.

2.6 Thermal Energy Order of Magnitude

For an aircraft phase i, a first-order estimate of heat released from fuel consumption is;

$$E_heat,i = m_f,i\ LHV\ \eta_h,i \quad (7)$$

where m_f,i is fuel consumed, LHV is the lower heating value of aviation fuel, and η_h,i is the fraction contributing to local sensible and radiative heating within the domain of interest. This expression is an order-of-magnitude constraint rather than a complete plume model. The spatial and temporal impact also depends on exhaust momentum, plume rise, aircraft speed, atmospheric stability, and advection.

2.7 Uncertainty

For independent uncertainty components, first-order propagation can be expressed as;

$$\sigma_y^2 \approx \Sigma_j\ (\partial f/\partial x_j)^2\ \sigma_xj^2 \quad (8)$$

For ΔLST, relevant terms include Landsat product uncertainty, pixel sampling variability, emissivity error, geolocation, cloud screening, reference-zone selection, and temporal mismatch between satellite and ground observations. A doctoral-level assessment should report confidence intervals or bootstrap distributions for ΔLST and τ_DID, together with sensitivity tests for alternative reference zones and activity thresholds.

2.8 Confirmatory Spatiotemporal Model

A doctoral-level confirmatory analysis should estimate the operational increment while allowing nonlinear meteorological responses and repeated observations within functional airport zones. A generalized additive mixed model can be written as;

$$T_{i,t} = \beta_0 + \beta_1\ I_LTO_{,i,t} + f_1(NDVI_i) + f_2(\alpha_i) + f_3(SW{\downarrow}_t) + f_4(U_t) + \beta_p P_t + u_i + v_t + \varepsilon_{i,t} \quad (12)$$

where $T_{i,t}$ is LST or near-surface air temperature at location i and time t; I_LTO is the phase-weighted exposure index; α_i is surface albedo; SW↓ is incoming shortwave radiation; U is wind speed or a wind-vector representation; P is rainfall or antecedent surface wetness; u_i and v_t are spatial and temporal random effects; and $\varepsilon_{i,t}$ is the residual. The coefficient β_1 represents the incremental operational signal after controlling for surface and atmospheric covariates. Smooth functions f_k permit nonlinear responses without imposing an unjustified linear relationship.

3. Study Area and Data

3.1 Luano Airport Setting

Lubumbashi/Luano International Airport (IATA: FBM; ICAO: FZQA) is located near 11°35′29″S, 27°31′52″E at an elevation of approximately 1309 m. The airport lies within the rapidly urbanizing Lubumbashi region of southeastern Democratic Republic of the Congo. The climate is tropical highland with a pronounced dry season, making it possible to contrast dry, strongly irradiated surface states with wetter periods in which evaporative cooling and cloudiness reduce the thermal signal.

3.2 Data Sources

Table 1 Data families and analytical roles

Data source	Variables	Role
Hourly meteorological observations	Air temperature, pressure, humidity, wind, rainfall	Local atmospheric state and quality control
Landsat 8/9 Collection 2 Level-2	Surface temperature, surface reflectance, NDVI, albedo proxies	High-spatial-resolution airport and reference-zone mapping
MODIS LST	Repeated thermal observations	Seasonal and interannual context
ERA5 reanalysis	Wind, temperature, humidity, radiation, stability proxies	Regional atmospheric background
CHIRPS	Precipitation, 2020-2024 products used in the primary study	Moisture-seasonality context
NASA POWER / regional climatology	Monthly temperature, rainfall, wind, radiation indices	Climatic favorability window
RVA operational traffic records	Arrivals, departures, time windows, operational phases	Activity classification and LTO exposure
Flightradar24 and FlightAware	Trajectory context and cross-checking	Spatial support where operational records permit

The source material includes representative products spanning different intervals: a Landsat thermal map dated 30 January 2025; NDVI products for March 2025-January 2026; precipitation aggregation for 2020-2024; albedo products for June-December 2025; NASA POWER climate fields for 2020-2025; and operational traffic windows derived from RVA records supplemented by commercial tracking platforms. Because these products are not temporally synchronous, the present manuscript treats them as a multiscale evidence base rather than as a single simultaneous experiment.

3.3 Quality-Control Requirements

- Apply Landsat Level-2 quality masks and exclude clouds, cloud shadows, and low-quality surface-temperature pixels.
- Maintain separate interpretations for LST and 2-m air temperature; do not convert one into the other without a validated transfer model.
- Match airport and reference zones by elevation, background urban influence, and surface class where feasible.
- Synchronize traffic events, meteorological observations, and satellite acquisition times in UTC.
- Conduct sensitivity analyses for active-hour thresholds, reference-zone geometry, and wind-sector stratification.
- Document missing traffic data and avoid treating commercial flight-tracking data as complete operational records.

4. Methods

4.1 Spatial Units

The analysis distinguishes the airport footprint from external reference areas and subdivides the airport into runway, taxiway, apron, parking, holding-point, terminal/technical, and trajectory-exposure zones. This functional zoning is essential because the expected operational perturbation is anisotropic rather than radial. Takeoff roll, initial climb, approach, landing, and apron activity occur along specific corridors and cannot be represented adequately by a single airport-average value.

4.2 Temporal Stratification

Each observation period is classified by season, day versus night, active versus idle traffic, rainfall history, and wind regime. The primary study identified a bimodal daily traffic pattern with a principal midday activity peak and a secondary late-afternoon peak. Comparisons should therefore be made within matched diurnal windows to avoid conflating traffic with the normal solar cycle.

4.3 Climate-Favorability Index

A normalized climate-favorability index can prioritize periods during which a localized LTO signal is most detectable:

$$CFI_m = w_R R^*_m + w_T T^*_m + w_W(1 - W^*_m) + w_P(1 - P^*_m) \quad (9)$$

where R*, T*, W*, and P* are normalized radiation, temperature, wind, and precipitation indices for month m, and the weights sum to one. The index is not an independent climatic truth; it is a transparent screening tool. The primary study indicates that June-September provides the most favorable combination of strong radiation, dry surfaces, low precipitation, and moderate dispersion conditions.

4.4 Interpretation Hierarchy

Evidence is interpreted in three hierarchical levels. Level 1 identifies a structural airport surface anomaly through persistent ΔLST and low vegetation. Level 2 tests whether thermal patterns are spatially aligned with functional airport zones and LTO exposure. Level 3 seeks temporal attribution through Eq. (6), synchronized ground observations, and uncertainty analysis. The existing publication strongly supports Levels 1 and 2, while Level 3 remains a research requirement because the necessary event-level regression outputs and uncertainty intervals were not reported.

4.5 Robustness, Sensitivity, and Attribution Tests

A confirmatory analysis should report sensitivity to (i) alternative airport and reference-zone geometries, (ii) active-hour definitions, (iii) wind-direction sectors, (iv) antecedent rainfall windows, (v) cloud and quality-screening thresholds, and (vi) exclusion of extreme-traffic or extreme-weather days. Placebo tests should assign pseudo-LTO events to idle periods, and event-study coefficients should be inspected for pre-event trends. Spatial block cross-validation should be used where regression or machine-learning models are fitted, because random pixel splits can overstate performance when neighboring pixels are autocorrelated.

5. Results

5.1 Persistent Surface Thermal Structure

The Landsat thermal product shows a marked warm core across the urbanized and airport sectors of Lubumbashi. Within the airport environment, the highest surface temperatures coincide with highly impervious and operationally intensive zones. The diachronic analysis summarized in the primary publication reported an increase of approximately 2.8°C over several decades. Because the underlying time series and formal trend uncertainty are not reproduced here, the value is interpreted as a descriptive long-term signal rather than as a fully quantified attribution to airport operations. The approximately 2.8°C diachronic increase reported in the source study is retained as a descriptive result; the complete time series, uncertainty interval, and attribution decomposition were not included in the supplied materials and therefore are not reconstructed here.

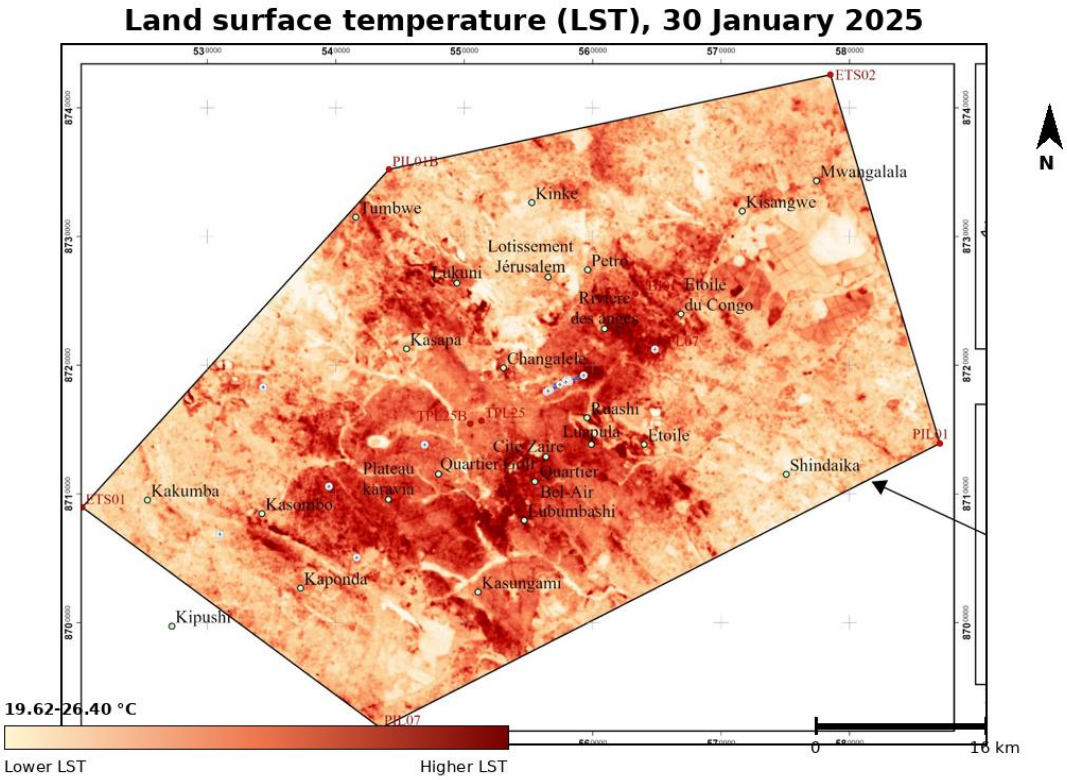

Fig. 2 Land surface temperature distribution over Lubumbashi and the Luano airport environment on 30 January 2025, based on Landsat 8 thermal products. The cartographic panel has been redrawn in English from the source study

5.2 Spatial Alignment with Aircraft Trajectories

Flight-trajectory mapping indicates that recurrent arrival and departure corridors intersect the thermally structured airport and urban environment. Spatial coincidence does not by itself demonstrate causation, because aircraft operate over surfaces that are already warm and artificialized. It does, however, identify where event-level measurements should be concentrated: runway thresholds, departure-roll segments, holding points, apron areas, and the first kilometers of climb.

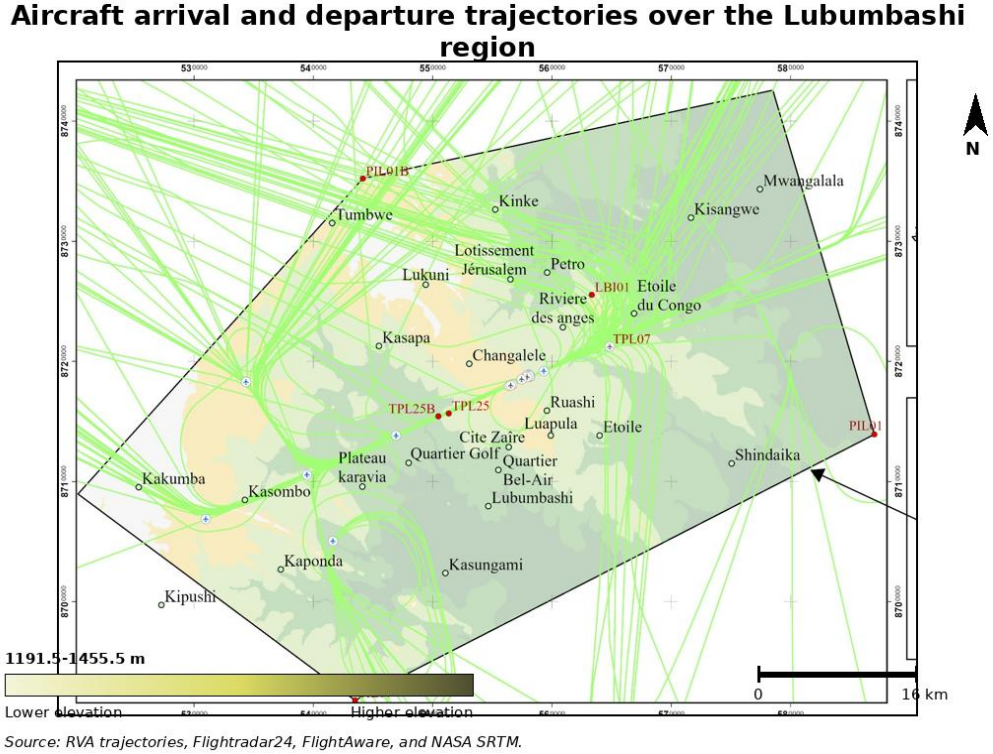

Fig. 3 Spatial distribution of aircraft arrival and departure trajectories in relation to relief and the thermally differentiated Luano-Lubumbashi environment. The panel has been redrawn in English from the source study

5.3 Vegetation Control

The NDVI map reveals a strong contrast between vegetated peripheral areas and the more artificialized airport and urban core. The spatial inverse relationship between NDVI and LST is consistent with reduced latent heat flux and increased sensible heating over mineral surfaces. This result supports the interpretation that the dominant background thermal signal is a land-surface signal rather than a direct traffic signal.

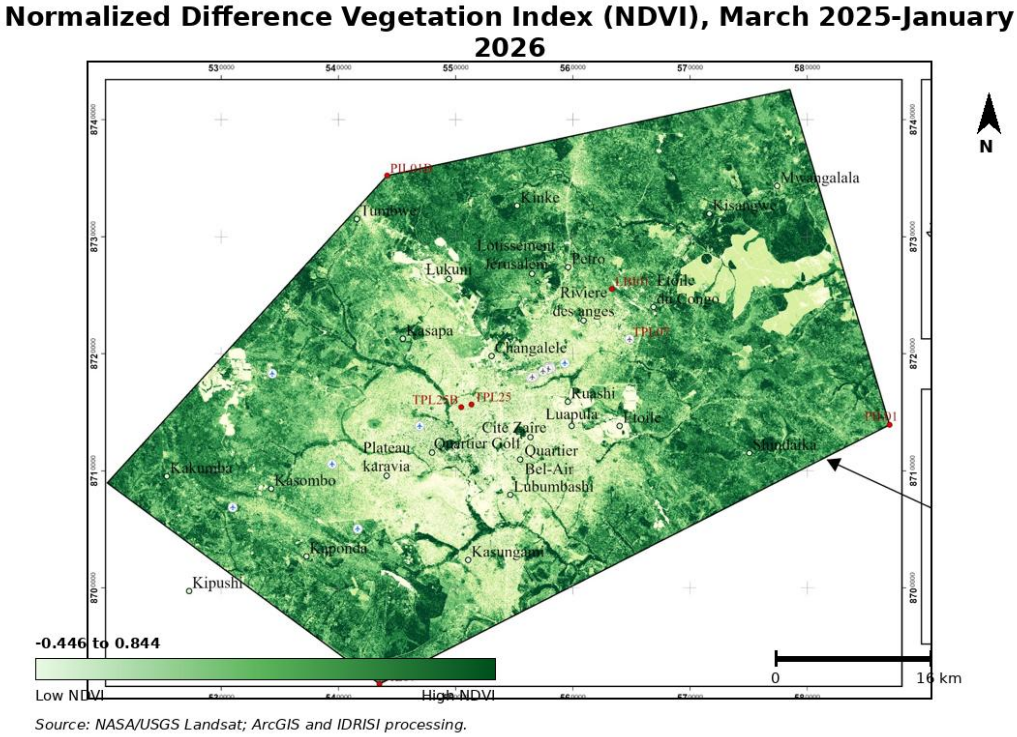

Fig. 4 Normalized Difference Vegetation Index (NDVI) for the Lubumbashi region, including Luano Airport, for March 2025-January 2026. Low NDVI over artificialized sectors is consistent with reduced evaporative cooling

5.4 Moisture, Albedo, and Seasonal Modulation

The precipitation field used in the primary publication indicates lower annual precipitation over the airport and central urban zone than over some peripheral sectors. The albedo product shows strong radiative absorption over the urban-airport surface complex. These results are physically consistent with a dry-season enhancement of surface thermal contrasts. The evidence should nevertheless be viewed as multiyear climatological context rather than as proof that urbanization caused the mapped precipitation gradient.

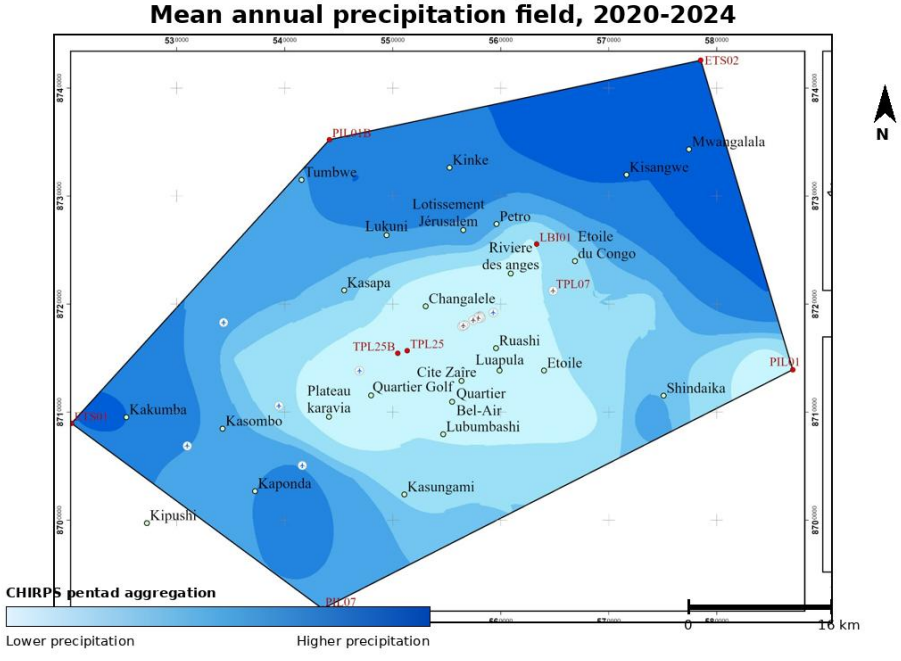

Fig. 5 Mean annual precipitation field for 2020-2024 from CHIRPS products. The pattern is used as a moisture and seasonality context; causal attribution of the gradient requires local gauge validation

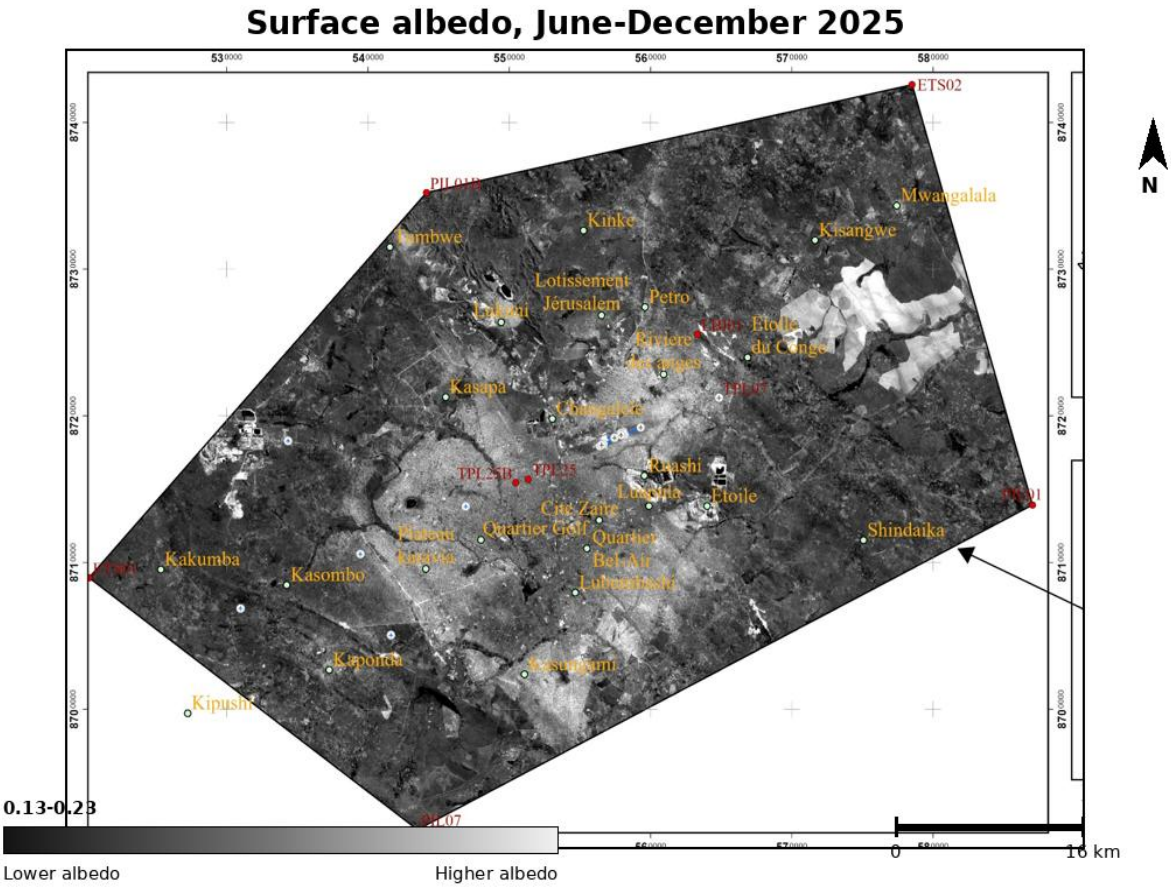

Source: NASA/USGS Landsat 8; ArcGIS and Python processing.

Fig. 6 Surface albedo distribution derived from Landsat products for June-December 2025. Lower-albedo surfaces absorb more shortwave radiation and can reinforce daytime surface heating

5.5 Climatic Windows and Traffic Timing

The monthly synthesis identifies the dry season, especially June-September, as the period with the greatest signal-to-noise ratio for detecting operational thermal increments. The traffic matrix indicates repeated active windows centered on midday and a secondary late-afternoon period. These windows overlap with high-radiation conditions, making matched active-idle comparisons essential. Without time-of-day control, the normal diurnal temperature cycle could be incorrectly attributed to LTO activity.

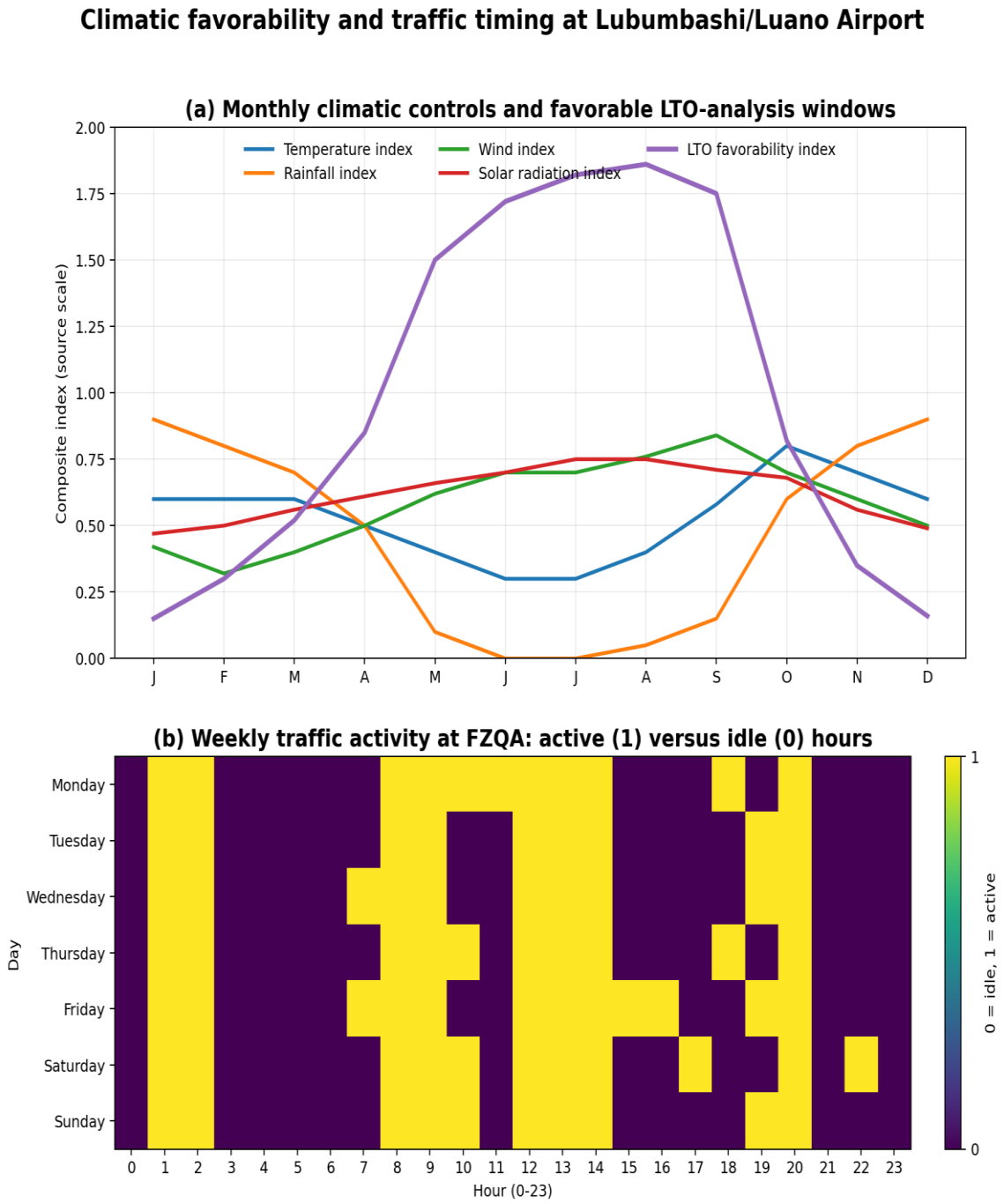

Fig. 7 Monthly climatic controls and weekly traffic timing. (a) Source climate indices and the composite LTO-favorability window. (b) Active (1) and idle (0) hourly traffic windows for arrivals and departures. The graphics have been redrawn in English from the source study

5.6 Wind and Anisotropy

Wind is a principal moderator. Stronger flow enhances advection and dispersion, reducing the duration of localized thermal and mechanical anomalies. Weak-to-moderate flow permits longer persistence but can also shift the anomaly downwind. The spatial climate product further shows that the environment is not homogeneous. Operational effects should therefore be analyzed by wind sector and functional zone rather than by airport-wide averages.

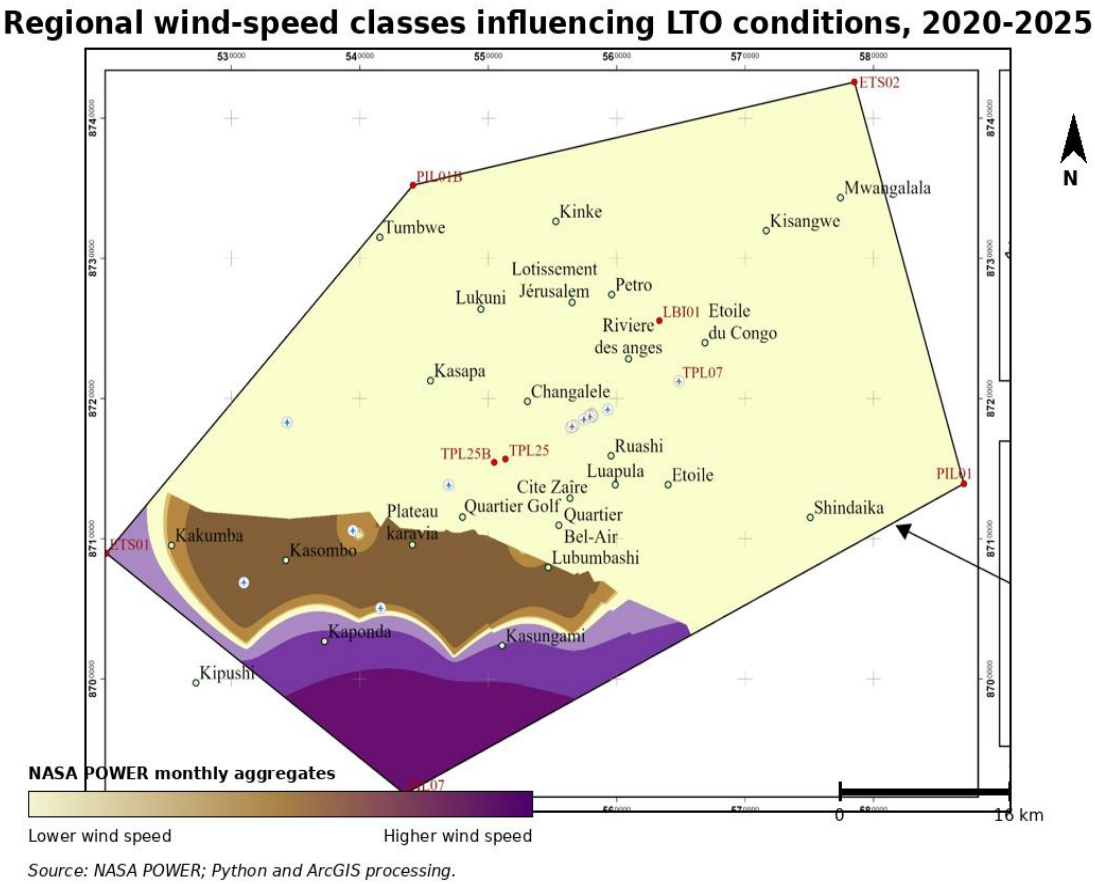

Fig. 8 Regional wind-speed classes influencing LTO-related dispersion and persistence in the Luano area, based on NASA POWER fields for 2020-2025 and redrawn in English

6. Discussion

6.1 Structural Airport Heat versus Operational Amplification

The strongest inference is that Luano possesses a structured airport-related surface thermal anomaly. The airport is warm because its surface is highly mineralized, its vegetative cooling is limited, and its materials absorb and store solar energy. LTO activity is superimposed on this background. Engine exhaust, jet momentum, auxiliary power use, ground vehicles, and braking or rolling processes can add localized thermal and mechanical forcing, but the available evidence does not support the claim that aircraft movements are the sole or dominant cause of the long-term surface-temperature increase. This interpretation is consistent with airport-infrastructure studies showing that impervious expansion and operational development can alter surface heat-island intensity over multiyear periods [23], [25]. The distinctive contribution of the Luano framework is to reserve a separate, testable term for short-duration LTO forcing instead of assigning the entire anomaly to airport operation.

This distinction is central to scientific attribution. The maps provide strong spatial evidence, while the active-idle framework provides a credible pathway for temporal attribution. A future study should estimate Eq. (6) from synchronized ground and traffic data, report uncertainty, test parallel pre-event behavior, and examine heterogeneity by aircraft class, phase, wind sector, and season. Until such estimates are available, LTO operations should be described as plausible and spatially coherent amplifiers rather than as a fully quantified causal contribution.

6.2 LST Is Not Air Temperature

Satellite LST characterizes the radiometric skin temperature of the surface. It can differ substantially from 2-m air temperature, especially under strong solar radiation, low wind, or heterogeneous urban geometry. Nichol et al. [15] and Voogt and Oke [21] emphasized the need to combine remote sensing with in situ measurements. The present study therefore interprets LST as a surface-energy indicator. Any operational statement about aircraft performance must ultimately use measured or properly modeled air temperature, pressure, and humidity, not satellite LST alone.

6.3 Multi-Source Strength and Temporal Mismatch

The multi-source design is a major strength because no single dataset can resolve surface properties, atmospheric state, and traffic simultaneously. Landsat provides detailed spatial structure, MODIS provides temporal context, ERA5 provides regional meteorological continuity, CHIRPS provides moisture-seasonality information, and operational records identify active periods. The corresponding limitation is temporal mismatch. A rigorous follow-on campaign should define a common analysis period, synchronize all observations, and separate exploratory mapping from confirmatory inference.

6.4 Generalizability

Luano is representative of a broader class of tropical and subtropical airports characterized by high elevation, strong dry seasons, expanding impervious surfaces, sparse local observations, and rapid urbanization. The analytical framework is transferable, but the estimated relationships are site specific. Airports with humid maritime climates, different runway orientations, stronger prevailing winds, or denser vegetation may display a weaker or differently shaped surface anomaly.

The regional significance is substantial. Many African airports combine rapid urban expansion, large mineralized surfaces, high solar loading, limited station density, and heterogeneous operational records. A reproducible airport-reference design can therefore support both environmental monitoring and the quality control of climate observations recorded at airport stations. Cross-airport comparison should use local climate zones, standardized buffer geometries, and common event definitions to avoid attributing differences in urban form or background climate to aviation activity.

7. Aviation and Operational Implications

7.1 Air Density and Aircraft Performance

Moist-air density can be approximated using virtual temperature:

$$\rho = p/(R_d T_v) \tag{10}$$

where p is pressure, R_d is the gas constant for dry air, and T_v is virtual temperature. At fixed pressure, increasing temperature reduces density. The aerodynamic lift relation

$$L = 0.5 \rho V^2 S C_L \tag{11}$$

shows that lower density requires higher true airspeed or other compensating changes to produce the same lift. Operationally, high density altitude increases takeoff distance and reduces climb performance, particularly at elevated airports [4]. The microclimate does not replace the official meteorological observation used for flight operations, but localized temperature heterogeneity can motivate improved sensor siting, runway-segment monitoring, and density-altitude awareness.

7.2 Low-Level Turbulence and Dispersion

Thermally driven convection above strongly heated surfaces can interact with jet exhaust, wake vortices, and terrain-induced flow. The source article does not provide turbulence measurements; therefore no quantitative turbulence increment is claimed. However, the spatial coincidence of hot surfaces, active movement zones, and variable wind supports the deployment of fast-response temperature, wind, and turbulence sensors near runway ends, holding points, and downwind sectors.

7.3 Environmental and Planning Implications

The findings support an airport environmental strategy that monitors recurrent hot zones, evaluates pavement optical properties, preserves operationally compatible vegetation, and integrates microclimate into infrastructure and safety assessments. Vegetation interventions must remain compatible with obstacle limitation, wildlife-hazard management, drainage, and security requirements. Reflective or lower-heat-storage materials may reduce surface temperature, but their glare, durability, friction, and maintenance implications require aviation-specific evaluation.

8. Validation Strategy for a Doctoral-Level Follow-On Study

Table 2 Minimum validation program for a confirmatory airport microclimate experiment

Component	Minimum design	Purpose
Near-surface air temperature	Shielded aspirated sensors at runway, apron, reference, and downwind sites	Resolve air-surface decoupling and local gradients
Surface temperature	Infrared radiometers plus Landsat/MODIS products	Validate radiometric LST and diurnal persistence
Wind and turbulence	3D sonic anemometers at critical zones	Measure advection, gusts, and turbulence kinetic energy
Aircraft operations	Time-synchronized RVA movement logs, aircraft/engine class, phase timing	Estimate phase-specific exposure and causal increments
Surface state	NDVI, albedo, moisture, material class	Control the structural thermal background
Statistical inference	Fixed-effects/DiD models, bootstrap intervals, sensitivity tests	Quantify τ_DID and uncertainty

A robust design should collect at least one full annual cycle, with intensified sampling during the dry-season detection window. Event studies should use pre-event, event, and post-event windows and should stratify by aircraft class, phase, and wind direction. Reference sensors should be positioned outside direct operational influence but within the same regional atmospheric regime. Statistical reporting should include effect sizes, 95% confidence intervals, residual diagnostics, cross-validation, and explicit treatment of missing movements and satellite cloud gaps. The preferred inferential unit is a synchronized space-time observation (sensor or pixel by hour). Power calculations should be based on the smallest operationally meaningful temperature increment and the observed autocorrelation structure rather than on independent-sample assumptions. Uncertainty should be reported separately for satellite retrieval, sensor calibration, temporal matching, traffic completeness, and model specification.

9. Limitations

- The English manuscript is a secondary publication and does not constitute a new independent dataset.
- The reported approximately 2.8°C diachronic increase is not accompanied here by the full time series, trend model, confidence interval, or attribution decomposition.
- Traffic records and commercial tracking sources may be incomplete; aircraft and engine-specific fuel-flow data were not reported. They may be included in future studies.
- LST is a surface variable and cannot substitute directly for 2-m air temperature or aircraft-experienced atmospheric conditions.
- The representative spatial products cover different time intervals and are not fully synchronous.
- The LTO exposure, difference-in-differences, uncertainty, and climate-favorability equations formalize the methodology but were not all empirically estimated in the primary publication.
- The maps have been redrawn in English from source cartographic products, they should be checked against the original GIS projects to have every legend class, scale, and metadata field.

10. Conclusions

Lubumbashi/Luano International Airport should be understood as a coupled surface-atmosphere-operations system. The available evidence supports a persistent airport-related surface thermal core associated primarily with impervious cover, reduced vegetation, moisture limitation, and radiative absorption. LTO cycles are best interpreted as localized, anisotropic, and transient amplifiers whose detectability depends strongly on wind, rainfall history, solar forcing, aircraft phase, and spatial proximity to operational corridors. This distinction prevents the structural airport heat island from being conflated with the incremental effect of aircraft activity.

The main methodological contribution is an integrated multiscale framework that combines an airport-reference LST contrast, a phase-weighted spatial LTO exposure field, climatic stratification, difference-in-differences, nonlinear spatiotemporal modeling, and explicit uncertainty propagation. The framework is scientifically defensible because it separates descriptive mapping from causal claims and specifies the observations required to test each mechanism. For tropical African airports, the approach offers a practical pathway from satellite-based screening to instrumented verification and operational risk assessment.

Acknowledgments

The authors gratefully acknowledge the academic supervision provided by Professor KABASELE YENGA YENGA Albert, PhD (Promoter), Professor FWAMBA MULUMBA Jean-Pierre (Co-promoter), and Associate Professor MINGA MILOLO Stéphane, PhD (Supervisor), Université Pédagogique Nationale, Kinshasa, Democratic Republic of the Congo. Their guidance contributed to the conceptual framing, scientific review, and doctoral supervision of this work. The authors also acknowledge the Régie des Voies Aériennes for operational aviation information and the providers of Landsat, MODIS, ERA5, CHIRPS, NASA POWER, and SRTM products. No external research funding was reported in the primary publication.

Data Availability Statement

Landsat, MODIS, ERA5, CHIRPS, NASA POWER, and SRTM data are publicly available from their respective providers. RVA operational traffic data are not publicly archived and may be accessed only subject to institutional authorization. Derived geospatial products may be made available by the corresponding author where licensing, security, and institutional rules permit.

Conflict of Interest

The corresponding author declare no conflict of interest.

Author Contributions

B. Diabasenga Kusuamina: conceptualization, aviation-operational framing, methodology, writing—original draft, and project coordination. A. Nzuzi Nzuzi: and S. Diabasenga Luyindula: civil-aviation data support, operational interpretation, and critical review. The academic supervisors named in the Acknowledgments provided doctoral guidance and scientific supervision.

Secondary Publication and Copyright Note

This manuscript is an expanded English-language secondary publication based on the French-language article entitled *"Dynamique microclimatique induite par les phases d'atterrissage et de décollage à l'aéroport international de Lubumbashi/Luano (RDC): Étude multi-scalaire couplant surface, atmosphère et opérations aéronautiques,"* previously published in the *International Journal of Innovation and Scientific Research*, Vol. 85, No. 1, June 2026, pp. 15–29.

The primary article was published under a Creative Commons Attribution licence, which permits reuse, adaptation, and redistribution provided that appropriate credit is given to the original authors and source. Copyright permission does not, however, replace the requirements of publication ethics. Accordingly, the present manuscript is explicitly identified as a secondary publication and not as an entirely independent original study.

The English version preserves the principal observations, datasets, figures, scientific interpretations, and conclusions reported in the primary publication. It extends the original work through a substantially revised international presentation, a more explicit surface–atmosphere–operations conceptual framework, additional mathematical formulations, a formal difference-in-differences approach, a spatiotemporal modelling framework, uncertainty propagation, expanded operational implications, and a doctoral-level validation strategy. No new empirical coefficient, statistical significance test, confidence interval, or causal effect estimate has been introduced unless directly supported by the available source data.

The French primary publication must be cited prominently in the manuscript and included in the reference list. The original article should also accompany the submission for editorial comparison. Submission of this English-language expanded version is subject to transparent disclosure of all overlapping material and, where required by the journals concerned, prior written approval from the editors of both the primary and secondary publications.

All authors have reviewed the relationship between the two publications, approved the present manuscript, and accept responsibility for the accuracy of the disclosure.

References

1. Arnfield, A. J., 2003: Two decades of urban climate research: A review of turbulence, exchanges of energy and water, and the urban heat island. Int. J. Climatol., 23, 1-26, https://doi.org/10.1002/joc.859.
2. Diabasenga Kusuamina, B., A. Nzuzi Nzuzi, and S. Diabasenga Luyindula, 2026: Dynamique microclimatique induite par les phases d'atterrissage et de décollage à l'aéroport international de Lubumbashi/Luano (RDC): Étude multi-

scalaire couplant surface, atmosphère et opérations aéronautiques [Microclimatic dynamics associated with aircraft landing and take-off phases at Lubumbashi/Luano International Airport]. Int. J. Innovation Sci. Res., 85, 15-29.
3. Earth Resources Observation and Science Center, 2020: Landsat 8-9 Operational Land Imager/Thermal Infrared Sensor Level-2, Collection 2. U.S. Geological Survey, https://doi.org/10.5066/P9OGBGM6.
4. Federal Aviation Administration, 2023: Pilot's Handbook of Aeronautical Knowledge. FAA-H-8083-25C, U.S. Department of Transportation.
5. Funk, C., and Coauthors, 2015: The climate hazards infrared precipitation with stations - a new environmental record for monitoring extremes. Sci. Data, 2, 150066, https://doi.org/10.1038/sdata.2015.66.
6. Gallo, K. P., J. O. Adegoke, T. W. Owen, and C. D. Elvidge, 2002: Satellite-based detection of global urban heat-island temperature influence. J. Geophys. Res. Atmos., 107, 4771, https://doi.org/10.1029/2002JD002588.
7. Gelaro, R., and Coauthors, 2017: The Modern-Era Retrospective Analysis for Research and Applications, Version 2 (MERRA-2). J. Climate, 30, 5419-5454, https://doi.org/10.1175/JCLI-D-16-0758.1.
8. Gough, W. A., and A. C. W. Leung, 2022: Do airports have their own climate? Meteorology, 1, 171-182, https://doi.org/10.3390/meteorology1020012.
9. Hersbach, H., and Coauthors, 2020: The ERA5 global reanalysis. Quart. J. Roy. Meteor. Soc., 146, 1999-2049, https://doi.org/10.1002/qj.3803.
10. Hulley, G. C., C. G. Hughes, and S. J. Hook, 2012: Quantifying uncertainties in land surface temperature and emissivity retrievals from ASTER and MODIS thermal infrared data. J. Geophys. Res. Atmos., 117, D23113, https://doi.org/10.1029/2012JD018506.
11. International Civil Aviation Organization, 2013: Airport Planning Manual. ICAO Doc 9184, Montreal, Canada.
12. Jin, M. S., 2012: Developing an index to measure urban heat island effect using satellite land skin temperature and land cover observations. J. Climate, 25, 6193-6201, https://doi.org/10.1175/JCLI-D-11-00509.1.
13. Lee, D. S., and Coauthors, 2021: The contribution of global aviation to anthropogenic climate forcing for 2000 to 2018. Atmos. Environ., 244, 117834, https://doi.org/10.1016/j.atmosenv.2020.117834.
14. Malakar, N. K., G. C. Hulley, S. J. Hook, K. Laraby, M. Cook, and J. R. Schott, 2018: An operational land surface temperature product for Landsat thermal data: Methodology and validation. IEEE Trans. Geosci. Remote Sens., 56, 5717-5735, https://doi.org/10.1109/TGRS.2018.2824828.
15. Nichol, J. E., W. Y. Fung, K. S. Lam, and M. S. Wong, 2009: Urban heat island diagnosis using ASTER satellite images and in situ air temperature. Atmos. Res., 94, 276-284, https://doi.org/10.1016/j.atmosres.2009.06.011.
16. Oke, T. R., 1987: Boundary Layer Climates. 2nd ed. Routledge, 435 pp.
17. Stewart, I. D., and T. R. Oke, 2012: Local climate zones for urban temperature studies. Bull. Amer. Meteor. Soc., 93, 1879-1900, https://doi.org/10.1175/BAMS-D-11-00019.1.
18. [18] Stull, R. B., 1988: An Introduction to Boundary Layer Meteorology. Kluwer Academic Publishers, 666 pp.
19. Tucker, C. J., 1979: Red and photographic infrared linear combinations for monitoring vegetation. Remote Sens. Environ., 8, 127-150, https://doi.org/10.1016/0034-4257(79)90013-0.
20. U.S. Geological Survey, 2021: Landsat Collection 2 Level-2 Science Products. USGS Fact Sheet 2021-3055, https://doi.org/10.3133/fs20213055.
21. [21] Voogt, J. A., and T. R. Oke, 2003: Thermal remote sensing of urban climates. Remote Sens. Environ., 86, 370-384, https://doi.org/10.1016/S0034-4257(03)00079-8.
22. Weng, Q., D. Lu, and J. Schubring, 2004: Estimation of land surface temperature-vegetation abundance relationship for urban heat island studies. Remote Sens. Environ., 89, 467-483, https://doi.org/10.1016/j.rse.2003.11.005.
23. Wan, J., B. Yong, and X. Zhou, 2022: Spatial and temporal analysis of the increasing effects of large-scale infrastructure construction on the surface urban heat island. Ecotoxicol. Environ. Saf., 237, 113521, https://doi.org/10.1016/j.ecoenv.2022.113521.
24. Yuan, F., and M. E. Bauer, 2007: Comparison of impervious surface area and normalized difference vegetation index as indicators of surface urban heat island effects in Landsat imagery. Remote Sens. Environ., 106, 375-386, https://doi.org/10.1016/j.rse.2006.09.003.
25. Ozenen-Kavlak, M., H. Duymus, G. B. Ozturk, S. Seyhan, S. N. Cabuk, and A. Cabuk, 2026: Determination of urban heat island effects of mega-scale infrastructure projects: Istanbul Airport-Istanbul Arnavutkoy region relationship. Environ. Sci. Pollut. Res., 33, 3379-3395, https://doi.org/10.1007/s11356-026-37469-6.
26. World Meteorological Organization, 2018: Guide to Instruments and Methods of Observation. WMO-No. 8, Geneva, Switzerland.